



$$\frac{R}{Q} = \frac{4\omega_r \mu A^2 \alpha_E^2}{(1 - 2\alpha_E(1 + Q)A^2)^2 + (1 - 2\alpha_E A^2)^2} \quad (6)$$

where  $\omega_r$  and  $Q_0$  are the resonant angular frequencies and the quality factor of the TE<sub>111</sub> mode,  $\alpha_E$  is the electrical polarizability of the single slot and the A coefficient is given by the following integral:

$$A = \frac{\omega_r L \tilde{J}_1(b)}{b\pi c} \left[ \int_b^a \frac{L\pi}{2} \left( k_i^2 (\tilde{J}_1)^2 r + \frac{(\tilde{J}_1)^2}{r} + \frac{k_i^4 L^2}{\pi^2} (\tilde{J}_1)^2 r \right) dr \right]^{\frac{1}{2}} \quad (7)$$

with  $\tilde{J}_1(r) = J_1(k_i r) - Y_1(k_i r) J_1'(k_i b) / Y_1'(k_i b)$ , the prime denote the total derivative with respect to the argument and  $k_i = \sqrt{(\omega_r/c)^2 - (\pi/L)^2}$ .

Considering the prototype dimensions, one obtains the values of  $\omega_r$ ,  $Q_0$  and  $R/Q$  reported in Table 2 (first column).

The value of the normalized power  $P_{Th}^{(0)} / Q_0 \tilde{J}_n^2$  as a function of  $r_0$  for  $\varphi_1 = 0$  is plotted in Fig. 2 and compared with the simulation and measurement results (described in the next section). In Fig. 3 the same quantity is plotted as a function of  $\varphi_1$  for  $r_0 = 0.6$  mm.

Table 2: theory, simulations and measurements results

	THEORY	HFSS	MEAS
$\omega_r$ [GHz]	3.78	3.74	3.74 (tunable)
$Q_0$	9600	9100	3500
$R/Q$ [mΩ]	36	31	39

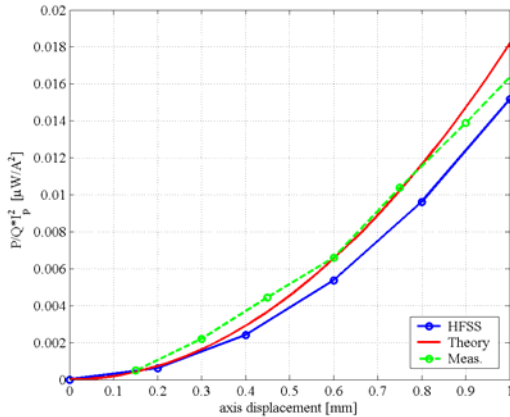


Figure 2:  $\underline{P}^{(0)} / Q_0 \tilde{J}_p^2$  as a function of  $r_0$  for  $\varphi_0 = 0$ .

### 3 SIMULATION RESULTS

To compare the analytical results with the numerical simulations, we have studied the coupling impedance of the cavity for the TE<sub>111</sub> mode as a function of the transverse displacement  $r_0$  and  $\varphi_1$ . We have, therefore, calculated the longitudinal shunt impedance of the mode ( $R_s$ ) for different axial positions, using the Eigenmode Solver of HFSS.

The HFSS model is shown in Fig. 4 with the obtained E field lines. It is only 1/8 of the structure with proper

magnetic and electric boundary conditions on the symmetry planes. The average dissipated power in the cavity corresponding to the TE<sub>111</sub> mode is given by:

$$P_{Sim}^{(0)} = \frac{1}{2} R_s (\varphi_1, r_0) \tilde{J}_n^2 \quad (8)$$

The value of  $P_{Sim}^{(0)} / Q_0 \tilde{J}_n^2$  is plotted in Figs. 2-3 and compared with the analytical and measurement results. From the previous plot it is possible to verify that it is possible to write the eq. (8) in the form:

$$P_{Sim}^{(0)} \equiv \frac{1}{2} \frac{R}{Q} Q_0 \cos(\varphi_1)^2 r_0^2 \tilde{J}_n^2 \quad (9)$$

The values of  $\omega_r$ ,  $Q_0$  and  $R/Q$  obtained by the simulations are reported in Table 2 (second column).

If the cavity is coupled through a small probe to an external load, then the average dissipated power in the system is still given by eq. (5) or (9) but with  $Q_0$  replaced by the loaded  $Q_L$ . The average power dissipated in the load ( $P_{Ext}^{(0)}$ ) is related to the power dissipated in the cavity by:

$$P_{Ext}^{(0)} = P_{cav}^{(0)} \beta / (1 + \beta) \quad (10)$$

where  $\beta$  is the coupling coefficients between the probe and the cavity mode TE<sub>111</sub> and it can be obtained from reflection measurement at the probe port.

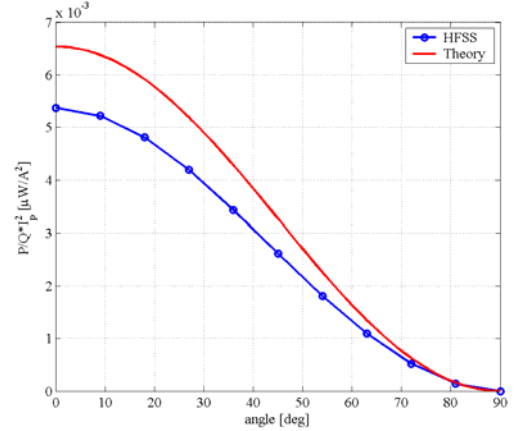


Figure 3:  $\underline{P}^{(0)} / Q_0 \tilde{J}_p^2$  as a function of  $\varphi_1$  for  $r_0 = 0.6$  mm.

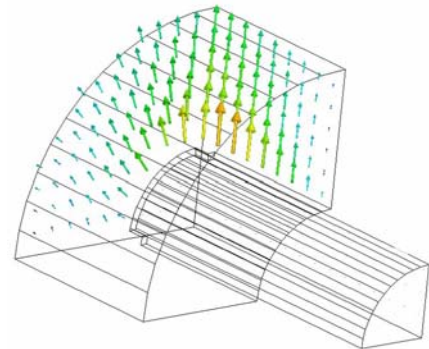


Figure 4: HFSS model with E field lines.

### 4 PROTOTYPE MEASUREMENTS

Wire measurements have been performed on the aluminum prototype shown on Fig. 5. An antenna probes the signal in the cavity.

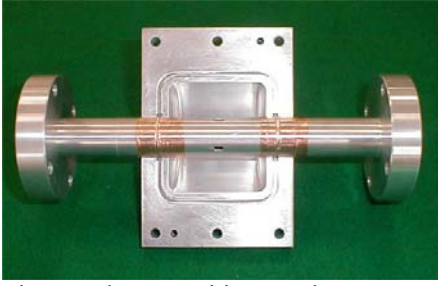


Figure 5: beam position monitor prototype.

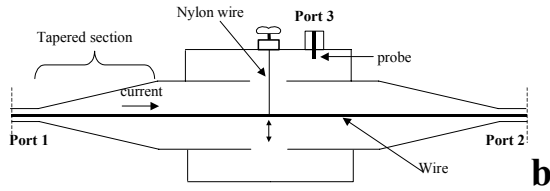
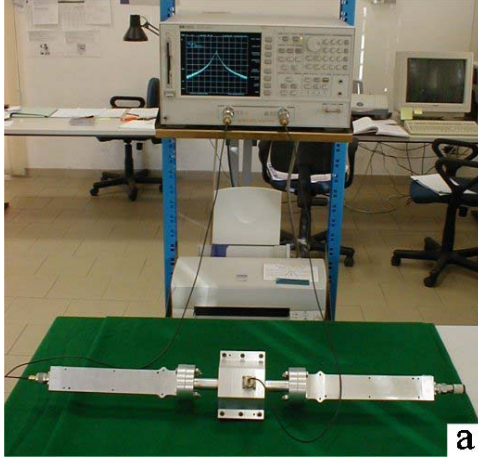


Figure 6: measurement setup

The measurements setup is shown Fig. 6a and schematically represented in Fig 6b. The wire has a radius of 1.5 mm. In order to minimize reflections at the ports 1 and 2 we have inserted two tapered sections that match the  $50 \Omega$  impedance of the Network Analyzer with the  $\sim 114 \Omega$  impedance of the wire in the beam pipe. To excite the dipolar mode  $TE_{111}$  the wire inside the beam pipe has been properly displaced from the axis of the beam pipe. To this purpose, a thin nylon wire has been connected to the wire in order to displace it from the beam pipe axis in a controlled way and to excite the polarity  $\varphi_0$ . The measured transmission coefficient  $S_{21}$  and  $S_{31}$  are shown in Fig. 7 for a displacement of the wire of  $\sim 1.5$  mm.

The average dissipated power in the cavity is given by:

$$P_{cav}^{(0)} = P_{Ext}^{(0)} \frac{(1+\beta)}{\beta} \cong \frac{1}{2} Z_c \frac{|S_{31}(\omega_r)|^2}{|S_{21}(\omega_r)|} \frac{(1+\beta)}{\beta} \tilde{I}_n^2 \quad (11)$$

The plot of  $P_{cav}^{(0)} / Q \tilde{I}_p^2$  as a function of  $r_0$  is reported in Fig. 2. It is clear that  $P_{cav}^{(0)}$  can be written in the form (5) or (9) and the equivalent R/Q is reported in Table 2. The Q factor of the resonant mode is lower than the theoretical one because of RF losses in the mechanical contacts. Similar considerations than those developed in [6] can be

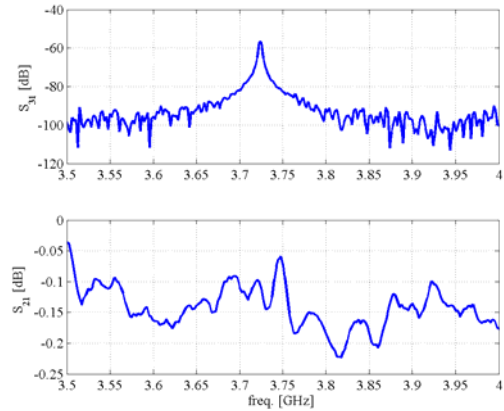
done from the point of view of the induced errors in the measurement setup.

By the system of equations (4) it is possible to calculate the position of the bunches in the beam pipe when the b.p.m is inserted in the accelerator, by the formulae:

$$\begin{cases} r_0 = \frac{\sqrt{P_{Ext}^{(\pi/2)} / \underline{P} + P_{Ext}^{(0)} / \underline{P}}}{\tilde{I}_n} \\ \varphi_1 = \pm \arctan \left( \sqrt{\frac{P_{Ext}^{(\pi/2)}}{P_{Ext}^{(0)}}} \right) \pm \pi \end{cases} \quad (12)$$

where the calibration coefficient  $\underline{P}$  is given by:

$$\underline{P} = \frac{1}{2} Z_c \frac{|S_{31}(\omega_r)|^2}{|S_{21}(\omega_r)|} \frac{1}{r_0^2} \quad (13)$$


 Figure 7: measured transmission coefficients ( $S_{12}$ ,  $S_{31}$ ).

## 5 CONCLUSIONS

A novel bunch position monitor has been described. Measurements on an aluminium prototype have been compared to the theoretical and numerical expectations of the power dissipated by the first dipolar mode in the cavity. The compare shows a good agreement between theory and simulations especially considering the mechanical differences between the prototype and the ideal structure. These results confirm the potential application of this device as a beam position monitor. The very low coupling impedance of the device and the possibility of calibration by simple wire measurements make the device hopefully usable in the accelerator machines.

## 6 REFERENCES

- [1] S. De Santis and L. Palumbo, *Phy. Rev. E*, vol 55, pp. 2052-2055, 1997.
- [2] C. D'Alessio, *Tesi di Laurea*, Univ. "La Sapienza", 2002.
- [3] <http://www.ansoft.com>
- [4] F. Caspers, in *Handbook of Accelerator physics and engineering*, pp. 570-574, World Scientific, 1999.
- [5] A. Hofmann, "Beam Instabilities", CERN 95-06, Geneva, 1995.
- [6] D. Alesini et al., *Proc. of EPAC 2002*, pp. 1834-1836, Paris